Remote Sensing in Ecology and Conservation
Open Access
ZSL LET'S WORK FOR WILDLIFE

ORIGINAL RESEARCH

How can Sentinel-2 contribute to seagrass mapping in shallow, turbid Baltic Sea waters?

Katja Kuhwald[1], Jens Schneider von Deimling[2], Philipp Schubert[3] & Natascha Oppelt[1]

[1]Earth Observation and Modelling, Department of Geography, Christian-Albrechts-Universität zu Kiel, Ludewig-Meyn-Str. 8, Kiel D-24098, Germany
[2]Marine Geophysics and Hydroacoustics, Institute of Geosciences, Christian-Albrechts-Universität zu Kiel, Otto-Hahn-Platz 1, Kiel D-24098, Germany
[3]Marine Evolutionary Ecology, GEOMAR Helmholtz Center for Ocean Research Kiel, Düsternbrooker Weg 20, Kiel D-24105, Germany

Keywords
Baltic sea, benthic habitat mapping, eelgrass, random forest, Sentinel-2, submerged aquatic vegetation

Correspondence
Katja Kuhwald, Earth Observation and Modelling, Department of Geography, Christian-Albrechts-Universität zu Kiel, Ludewig-Meyn-Str. 8, Kiel D-24098, Germany. Tel: +49-431-880-5642; Fax: +49-431-880-4658; E-mail: katja.kuhwald@geographie.uni-kiel.de

Editor: Kylie Scales
Associate Editor: Vincent Lecours

Received: 18 August 2021; Revised: 7 November 2021; Accepted: 22 November 2021

doi: 10.1002/rse2.246

Remote Sensing in Ecology and Conservation 2022;**8** (3):328–346

Abstract

Seagrass meadows are one of the most important benthic habitats in the Baltic Sea. Nevertheless, spatially continuous mapping data of *Zostera marina*, the predominant seagrass species in the Baltic Sea, are lacking in the shallow coastal waters. Sentinel-2 turned out to be valuable for mapping coastal benthic habitats in clear waters, whereas knowledge in turbid waters is rare. Here, we transfer a clear water mapping approach to turbid waters to assess how Sentinel-2 can contribute to seagrass mapping in the Western Baltic Sea. Sentinel-2 data were atmospherically corrected using ACOLITE and subsequently corrected for water column effects. To generate a data basis for training and validating random forest classification models, we developed an upscaling approach using video transect data and aerial imagery. We were able to map five coastal benthic habitats: bare sand (25 km²), sand dominated (16 km²), seagrass dominated (7 km²), dense seagrass (25 km²) and mixed substrates with red/ brown algae (3.5 km²) in a study area along the northern German coastline. Validation with independent data pointed out that water column correction does not significantly improve classification results compared to solely atmospherically corrected data (balanced overall accuracies ~0.92). Within optically shallow waters (0–4 m), per class and overall balanced accuracies (>0.82) differed marginally depending on the water depth. Overall balanced accuracy became worse (<0.8) approaching the border to optically deep water (~ 5 m). The spatial resolution of Sentinel-2 (10–20 m) allowed delineating detailed spatial patterns of seagrass habitats, which may serve as a basis to retrieve spatially continuous data for ecologically relevant metrics such as patchiness. Thus, Sentinel-2 can contribute unprecedented information for seagrass mapping between 0 and around 5 m water depths in the Western Baltic Sea.

Introduction

Seagrass grows on soft sediments and is widely distributed in subtropical, temperate and even arctic waters. Seagrass meadows are the largest submerged aquatic vegetation ecosystem protected in Europe providing essential ecosystems for marine life as feeding ground, shelter, nursery and habitat (Short et al., 2016). They protect the coast by attenuating wave energy and trapping sediments (Orth et al., 2006); combined with nutrient uptake and pathogen reduction, they therefore improve near-shore water quality (Lamb et al., 2017; Short et al., 2007). As blue carbon ecosystems, seagrass meadows significantly store organic carbon in the underlying sediments for millennial timescales (Ricart et al., 2020; Lovelock & Duarte, 2019). Recently, the UNEP (United Nations Environment Programme) summarized how valuable seagrasses are to the environment and people (UNEP, 2020) Nevertheless, seagrass meadows retreat globally mainly due to eutrophication, diseases, coastal modifications and rising water temperatures (Los Santos et al., 2019; Waycott et al., 2009). Seagrass meadows react sensitively to changing

environmental conditions. Thus, they are well suited to indicate ecological status and health of coastal ecosystems (Madden et al., 2009); they therefore form a key quality element in the European Water Framework Directive (Marbà et al., 2013). Assessment of spatial and temporal dynamics demands dedicated mapping methods. The submerged nature of most seagrass species implies challenging conditions for optical approaches given the attenuation and turbidity of seawater (McKenzie et al., 2020). To map seagrass distribution, presence or absence and area extent are straightforward indicators (e.g. Lyons et al., 2013), while coverage is often used to map seagrass abundance (Borum et al., 2004). At micro- to mesoscale (<1 km²), divers map data for these indicators at predefined spots. Mappings with under-water video recording cover larger regions at the macro-scale (up to 100 km²). Both, video and traditional transect-diving provide point-based snapshots of the coastal ground (Borum et al., 2004; Schubert et al., 2015). Beyond a critical water depth, sunlight is hardly available and acoustic methods come into play for seagrass mapping with vessel mounted or towed sonar systems (Gumusay et al., 2019; Held & Schneider von Deimling, 2019). However, acoustic surveying is expensive especially in shallow water given its inverse relation between coverage per time and water depth. Therefore, shallow areas often remain uncharted and are often referred to as the uncharted 'coastal white ribbon' (Carvalho et al., 2017).

Airborne and spaceborne optical remote sensing can help to fill the data gap of the coastal white ribbon (<8 m water depth) at spatial scales >100 km² (McKenzie et al., 2020). Veettil et al. (2020) provide a comprehensive review of remote sensing for seagrass mapping. Commercial sensors with a very high spatial resolution, such as World-View-2, enable accurate mappings at metre scale (e.g. Kovacs et al., 2018). Freely available, for example Landsat data, allow time series back to the 1980s, but resolve spatially coarser with 30 m and less (e.g. Topouzelis et al. 2018). The launch of Sentinel-2 initiated seagrass mapping studies at spatial resolutions of 10–20 m, e.g. to map *Posidonia oceanica* in the Mediterranean Sea (Traganos & Reinartz, 2017, 2018) or to map different seagrass habitats in Australian waters (Kovacs et al., 2018). Combined with cloud computing, Sentinel-2 is potentially suited to map seagrass at continental to global scales (Traganos et al., 2018). These previous studies, however, were conducted in clear waters, where the maximum detection depth was around 20 m. Investigating Sentinel-2's capabilities for mapping seagrass also in turbid waters paves the way for global assessments. Wilson et al. (2020) and Zoffoli et al. (2020) carried out first attempts using Sentinel-2 for eelgrass and dwarf eelgrass (*Zostera marina, Zostera noltei*). The first successfully distinguished presence and absence of eelgrass in the complex, temperate waters of Atlantic Canada, while the latter assessed its seasonal variability along the European Atlantic coast. Zoffoli et al. (2020) focused on intertidal seagrass and therefore left the influence of the water column on the bottom signal unaddressed. Wilson et al. (2020) did not correct for the influence of the water column, although Traganos and Reinartz (2017) reported the correction as beneficial even for clear waters. No study, however, is available for analysing the potential of Sentinel-2 for mapping seagrass in the turbid waters of the Baltic Sea (Secchi disc depth between 2 m and >7 m; Stock, 2015), although it is considered as an ideal study area for marine and coastal ecosystem management (Reusch et al., 2018). The question of whether a water column correction improves seagrass monitoring in turbid waters also remains unanswered. The same applies to the question of whether mapping accuracies depend on the water depth.

With our study, we therefore aim to answer the following research questions:

How can Sentinel-2 contribute to fill data gaps to map seagrass in shallow, turbid waters of the Baltic Sea?
Do we need a water column correction to map seagrass accurately?
How do classification accuracies vary with water depth?

Due to its benthic characteristics and available validation data (chapter 2.2), the coastline of the northern German state 'Schleswig-Holstein' suits well to investigate Sentinel-2's capabilities for mapping seagrass in the Baltic Sea. In the following, we first describe how we scaled the in situ data to Sentinel-2 spatial resolution. After the atmospheric correction and masking of the Sentinel-2 data, we provide details on the approach to correct the water column, which is a modified version of Traganos and Reinartz (2017) clear water approach. Then, we classified benthic habitats based on water column corrected and non-corrected data. Afterwards, we validate the results water depth-dependently and discuss the research questions according to the limitations and potentials for seagrass mapping in the Baltic Sea.

Materials and Methods

Study area

The Baltic Sea is a semi-enclosed marginal sea with relatively little salt-water inflow from the North Sea and predominating freshwater inputs making it the largest brackish water system in the world. Water chemistry and optics strongly vary spatially in the Baltic Sea (Snoeijs-Leijonmalm & Andrén, 2017), which is known as turbid

(Kratzer & Moore, 2018). The study area is located in the Western Baltic Sea and covers about 240 km coastline of the northern German state 'Schleswig-Holstein' (Fig. 1). For Baltic Sea conditions, offshore waters of the selected study area are relatively clear with Secchi disk depth of about 5–6 m (MELUND 2017) during summer months. Winds, waves, bathing activities or boat traffic may resuspend sediments or organic matter locally and lead to increased turbidity in near-shore waters. This near-shore zone extends between 100 m and 2 km from the shoreline.

In the study area, large seagrass (*Zostera marina*) is the predominating seagrass species, which experienced significant changes during the last hundred years. European Zostera meadows declined sharply within the 20th century (Los Santos et al., 2019). In the Western Baltic Sea, various restoration efforts have been undertaken, but the meadows recover only slowly (Krause-Jensen et al., 2021). *Zostera marina* has been reported to grow down to 14 m in the Western Baltic Sea (Reinke, 1889; Schramm, 1996). In the German study area, video-based mapping activities and spatial distribution modelling show, that nowadays *Zostera marina* grows in patches and in sheltered areas as larger meadows on the mainly sandy ground only down to 8.5 m (Schubert et al., 2015), occasionally also on muddy sediments. Due to rising eutrophication levels, opportunistic algae may spread into seagrass habitats. Additionally, mixed habitats may occur with macroalgae (*Fucus spp.*, *Ceramium spp.*), cobbles, boulders or blue mussels (*Mytilus edulis*) in various fractions (Rönn et al., 2021; Schubert et al., 2015). The in situ data basis makes the area a suitable study area for optical and acoustic bathymetry (e.g. Niemeyer et al., 2015) and submerged vegetation analyses (Held & Schneider von Deimling, 2019; Schneider von Deimling, 2020).

Satellite data

Sentinel-2 carries the MultiSpectral Imager (MSI) with 13 bands in the visible, near-infrared and short-wave infrared

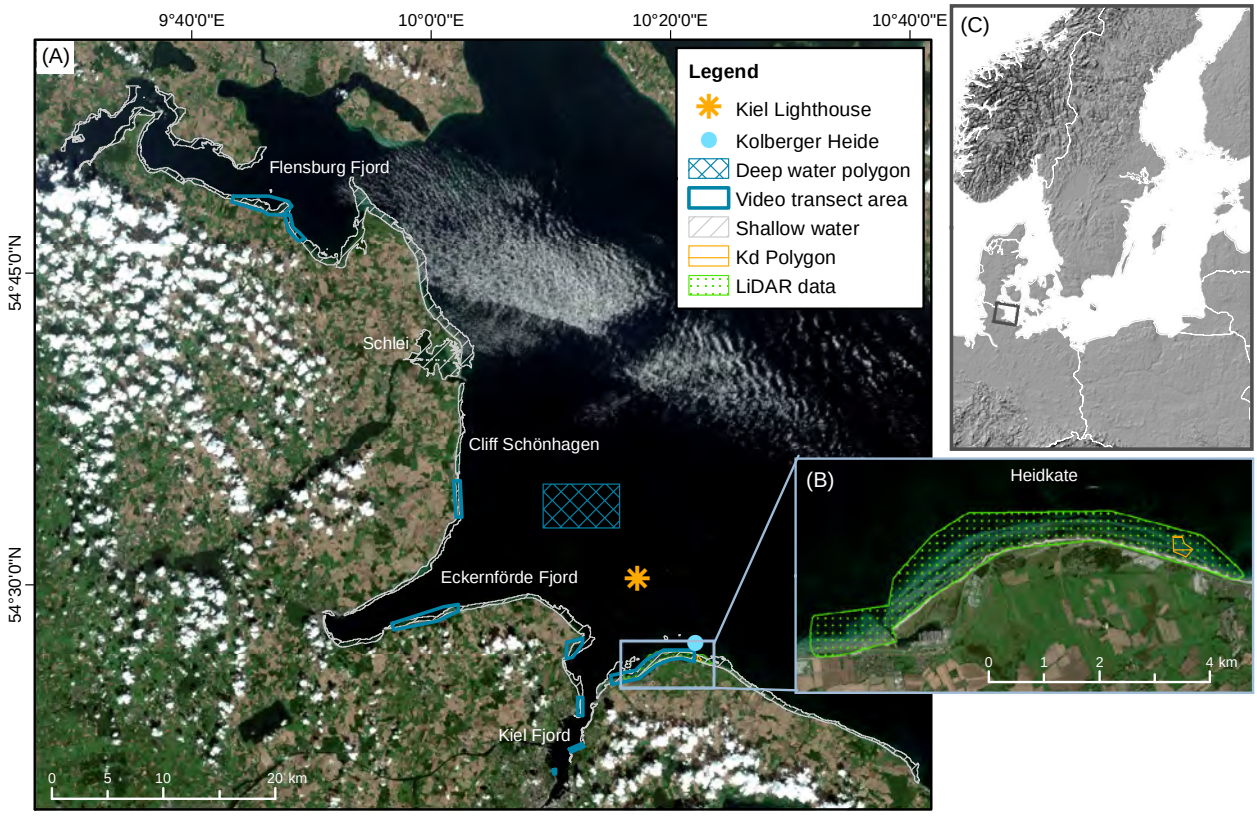

Figure 1. Overview of the study area along the Baltic Sea coast of Schleswig-Holstein with locations of measure data points (Kiel Lighthouse, Kolberger Heide), the analysed shallow water area and areas with video transect data (A). Background: Sentinel-2B True-Colour Composite 23rd Aug 2018 projected in UTM Zone 32 N/ WGS84. Detailed view of Heidkate where the LiDAR data were acquired (B). The location of the study area within the Western Baltic Sea (C).

wavelength region, which sample at three different spatial resolutions (10, 20 and 60 m) (Drusch et al., 2012). We downloaded one Sentinel-2B Level 1C scene (Processing baseline: 02.05, tile: 32UNF, relative orbit: 108) acquired during seagrass peak growth on 23th Aug 2017 from the Copernicus Open Access Hub. This mostly cloud-free image was closest to a LiDAR (Light Detection and Ranging) bathymetric survey conducted in the study area on 1st Sep 2017. Since the water column correction requires bathymetric data, the time offset of satellite and LiDAR data should be as small as possible to ensure comparable seabed conditions.

Coastal benthic habitats data

We used two different data sources to obtain information on coastal benthic habitats: (i) under-water video transect mappings and (ii) aerial true-colour ortho-photographies from the state agency for surveying and geoinformation Schleswig-Holstein (LVermGeo SH 2016). The LLUR (State agency for Agriculture, Environment andRrural Areas Schleswig-Holstein) and the GEOMAR Helmholtz Centre for Ocean Research cooperated to conduct under-water video transects mappings along the Baltic coastline of Schleswig-Holstein during summer months 2018–2020 following the methods in Schubert et al. (2015). A small workboat pulled a towed video camera about 1–2 m above the seafloor along the 4 m bathymetric contour. Additional videos were recorded perpendicular to the contours giving rise to vertical transects covering areas between 1 and 14 m water depth. Analysts interpreted the video imagery manually and assigned georeferenced points with the respective seagrass coverage value (0–100%).

Point data are problematic to calibrate and validate spatial mapping algorithms. We therefore selected patches of homogenous benthic habitats, with at least three times the smallest pixel size of Sentinel-2 (Dekker et al., 2011), that is 30 × 30 m. Following an upscaling approach, we combined the video points and true-colour aerial imagery (spatial resolution 0.2 m) acquired during summer 2016 (LVermGeo SH 2016). Local experts confirmed that changes in seagrass meadows are negligible within the time of in situ, airborne and space-borne data (2016–2019). We manually digitized polygons of clearly identifiable class patches based on the aerial imagery using QGIS (Version 3.12.0). The video points helped to verify the texture and colour patterns, which we associated with five habitat classes, that is dense seagrass, seagrass dominated, sand dominated, bare sand and mixed substrates with red/ brown algae. We then rasterized the digitized polygons to fit the Sentinel-2 10 m pixel grid (Fig. 2).

Bathymetric data

We selected shallow water areas (0–5 m) based on the official bathymetric raster (BSH, 2012). We additionally analysed bathymetric LiDAR water depths to calibrate and validate a scene-specific bathymetry model. Under the umbrella of the BONUS ECOMAP (Baltic Sea environmental assessments by innovative opto-acoustic remote sensing, mapping and monitoring) habitat mapping project (Schneider von Deimling, 2020), an airborne LiDAR (sensor: Riegl Q-820-G, flight height: ~500 m) campaign was conducted on 1st Sep 2017. The operating company 'DiMAP' processed the data using the software RiProcess and RiHydro. We conducted final spline filtering with the bathymetric postprocessing software Qimera (QPS). The LiDAR points have a horizontal spatial resolution of *c.* 1 m and were rasterized (arithmetic mean and standard deviation) to the Sentinel-2B grid (pixel size = 10 × 10 m). The tidal range is negligible in the study area and water levels measured at Kiel lighthouse were similar on the day of Sentinel-2B (23rd Aug 2017) and LiDAR data acquisition; we, therefore, omitted correcting water levels.

Methodology

Figure 3 schematically illustrates the data and processing steps. We conducted pre-processing with SNAP (version 8.0), QGIS (version 3.12) and Python (version 3.7). Python code and necessary data to run the script and reproduce the results are publicly available via Zenodo under the CC BY 4.0 license (https://zenodo.org/record/5212257#.YRv4iYgzZaQ; https://doi.org/10.5281/zenodo.5212256).

Table 1 lists the used Sentinel-2 bands with their spatial resolution. The central wavelengths correspond to the output of the used atmospheric correction algorithm ACOLITE.

Atmospheric correction and image masking

We applied ACOLITE (version v20210114.0) as an atmospheric correction algorithm, which is specifically designed for water bodies, to retrieve water-leaving remote sensing reflectance R_{rs} (sr^{-1}) (Vanhellemont, 2019). We applied the implemented 'dark spectrum approach' and also used the optional sun glint correction (Harmel et al., 2017). The resulting products are R_{rs} [sr^{-1}] with a 10 × 10 m pixel size, whereas values of 20 and 60 m bands are duplicated. Due to insufficient automatic cloud removal, we masked thin clouds in the northern part of the study area manually. For subsequent processing, we used the five bands between 442 and

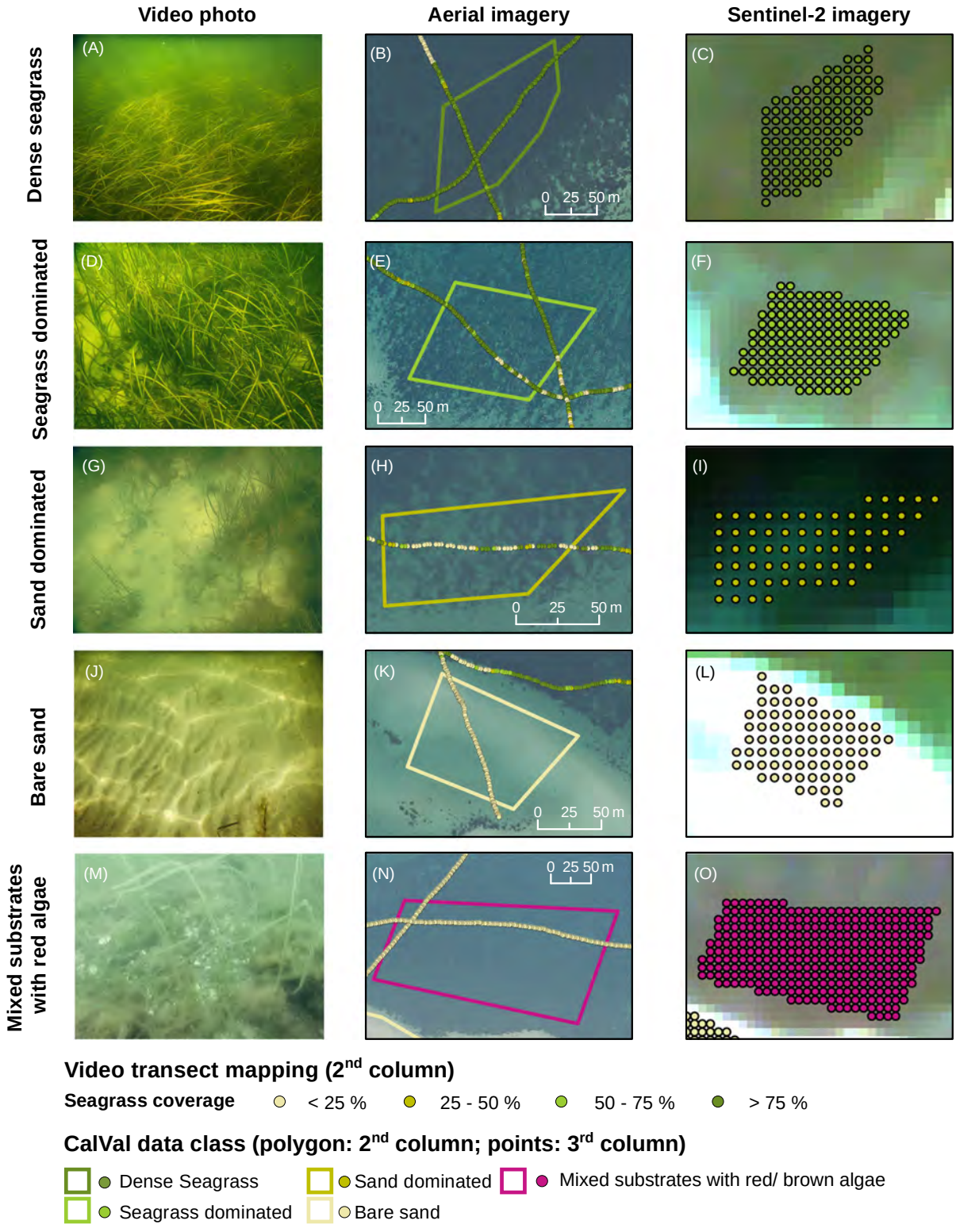

Figure 2. The five considered benthic habitat classes dense seagrass (A–C), seagrass dominated (D–F), sand dominated (G–I), bare sand (J–K) and mixed substrates with red/ brown algae (M–N). The 1st column illustrates how a class appears at the seafloor. The 2nd column indicates the upscaling approach of point-based video interpretation to polygons using aerial imagery (©GeoBasis-DE/LVermGeo SH). The background of the 3rd column is a true-colour composite of the ACOLITE-corrected Sentinel-2 scene of 23rd Aug 2017.

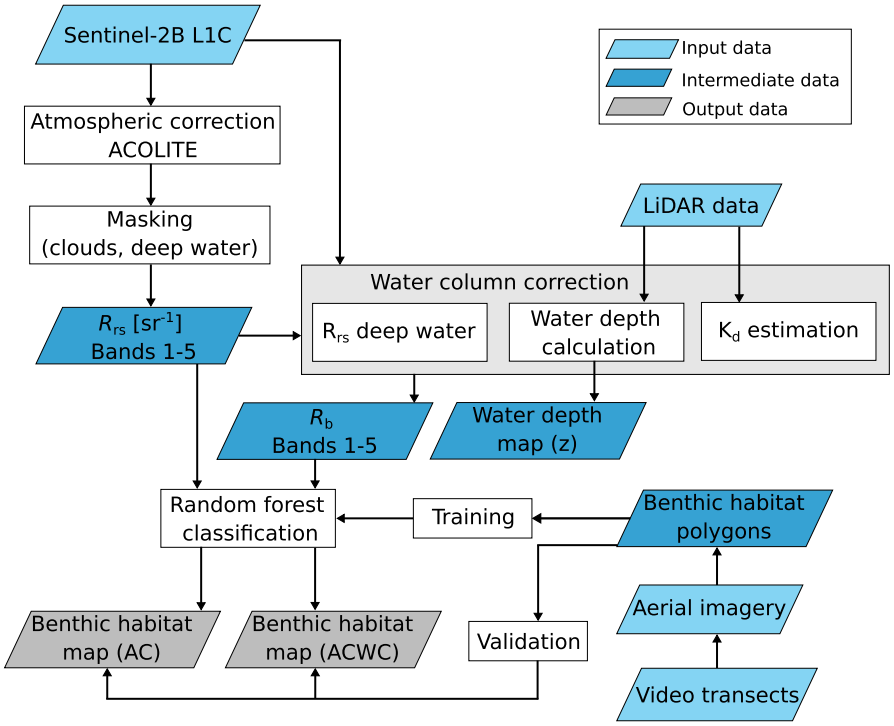

Figure 3. Schematic overview of the methodological framework and used data. L1C data correspond to the originally downloaded Sentinel-2 imagery at ESA Datahub. R_{rs} is the water-leaving remote sensing reflectance as output of the ACOLITE atmospheric correction. R_b bis the bottom reflectance after applying several processing steps. K_d corresponds to the diffuse attenuation coefficient. AC indicates the resulting map based on atmospherically corrected data (R_{rs}) and ACWC is based on atmospherically and water column corrected data (R_b).

Table 1. Spectral and spatial characteristics of the used Sentinel-2 bands.

Band no.	Central wavelength (ACOLITE) [nm]	Native spatial resolution [m]
1	442	60
2	492	10
3	559	10
4	665	10
5	704	20

704 nm (B1-B5). To reduce image noise, we applied a 3 × 3 mean filter to each band.

Water column correction

In optically shallow waters, four major components define R_{rs}, that is bottom reflectance R_b, water depth z and the inherent optical characteristics of the water body itself. The latter can be described by the diffuse attenuation coefficient K_d as well as absorption and scattering by optically active water constituents (Gege, 2017). R_b contains the information on benthic habitat classes. To retrieve R_b, we modified an image-based approach of Traganos and Reinartz (2017). This approach was developed in clear Mediterranean waters based on an analytical model of Maritorena et al. (1994). The following steps describe how we adapted the clear water approach (2017) to the more turbid conditions in the Baltic Sea.

Equation 1 represents the underlying model by Maritorena et al. (1994).

$$R_{rs}(\lambda) = R_{\mathrm{deep}}(\lambda) + \left(R_b(\lambda) - R_{\mathrm{deep}}(\lambda)\right) \bullet e^{(-2 \bullet K_d(\lambda) \bullet z))} \quad (1)$$

To obtain R_b, we have to estimate the wavelength-dependent water-leaving reflectance of deep water (R_{deep}), K_d, and the water depth z.

Reflectance of deep water R_{deep}

The oceanographic setting is relatively homogenous in the study area. We therefore assume that the water body (e.g. turbidity, optically active constituents) does not significantly change over the small distances in the specific area. Thus, R_{deep} can be used as a proxy to quantify the background signal of the water itself. To obtain R_{deep}, we selected a homogenous 6.8 × 3.9 km large area in optically deep waters of the study area (Fig. 1A, blue rectangle). The R_{deep} spectrum (Fig. 5) is the arithmetic mean of all spectra within this polygon.

Diffuse attenuation coefficient K_d

Here, K_d quantifies how radiation diminishes in the water column in both vertical directions, that is upwelling and downwelling. The intensity depends on the wavelength and regional optical properties of the water column. Generally, K_d increases with longer wavelengths (Kirk, 2011). Image-based K_d estimation requires an area with known, varying water depths, homogenous substrate and water column characteristics (Bierwirth et al., 1993; Traganos & Reinartz, 2017). To fulfil these requirements, we selected a sandy area of 805 pixels in the southeast of our study area, which covers depths between 0.8 and 4.2 m (Fig. 1B, orange poylgon). Following the proposed approach, we linearly correlated LiDAR retrieved water depths and R_{rs} of the Sentinel-2 bands 1–5 (442–704 nm). K_d can be calculated based on the slope (s) of each band's regression equation using Equation 2.

$$K_d = \frac{s}{-2} \quad (2)$$

Water depth z

If georeferenced water depths are available locally, scene-specific empiric models can be calibrated to retrieve water depths from Sentinel-2 imagery in optically shallow waters over large areas (Casal et al., 2018). Shallow water R_{rs} decreases exponentially with increasing water depths. Varying bottom coverages with non-vegetated and vegetated ground, however, often disrupt strong relationships. Compared to, for example sandy ground, vegetated areas reflect less at the same water depth since aquatic plants absorb incoming solar radiation (Kirk, 2011). Thus, we evaluated several band ratio and single-band models based on randomly selected 700 pixel pairs of the logarithmic R_{rs} and the LiDAR data to develop an empiric linear regression model bathymetry model. Alternatively, random forest and support vector machine regression models can be developed (e.g. Thomas et al., 2021). A single band model based on band 4 (665 nm) turned out to be best suited (R^2 = 0.75, Fig. 4). To verify how accurate the empiric model is, we calculated accuracy measures (R^2, RMSE) based on 300 independently and randomly selected data pairs. To obtain areal water depths in the study area, we applied the validated, scene-specific bathymetry model to Sentinel-2 band 4 (665 nm).

Benthic habitat classification and validation

Considering the spatial information available for benthic habitat classes and Sentinel-2's spectral and spatial characteristics, we identified five benthic habitat classes (Table 2), which are prevalent in the study area in water depths between 0 and 5 m. Nevertheless, small patches of less common benthic habitats may mix within the vegetation classes, such as *Fucus spp.*, *Mytilus edulis* or algae occurrences.

To map the benthic habitat classes, we implemented a random forest classifier using the python packages sklearn (version 0.24.1, Pedregosa et al., 2011) and pyimpute (version 0.2, Perry, 2020). The random forest classifier is a supervised ensemble classifier, which develops multiple decision trees (pre-defined number) based on randomly selected sub-samples of a training data set. According to its classification model, each tree classifies unknown pixels into a class. Finally, the results of all trees will be merged and the classifiers assign the class with most votes (Belgiu & Drăguţ, 2016; Traganos & Reinartz, 2017). To train and validate the classifier, we randomly split around 23 000 benthic habitat pixels into 70% training and 30% validation data. We trained and validated one random forest classifier with bands 1–5 using the R_b data (atmospheric + water column correction = ACWC) and a

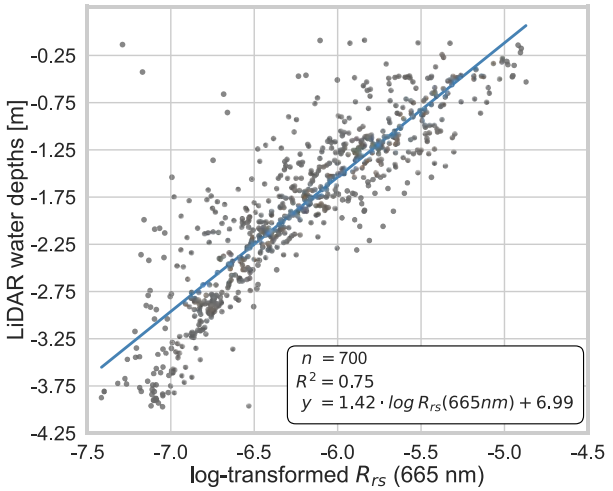

Figure 4. Scatterplot, linear regression line and equation between LiDAR-derived water depths and logarithmic R_{rs} of Sentinel-2 band 4 (665 nm) based on training data.

Table 2. Summary of the target benthic habitat classes.

Class	Description
Dense seagrass	>90% seagrass coverage in the pixel
Seagrass dominated	>50% seagrass, <50% sand coverage in the pixel
Sand dominated	<50% seagrass, >50% sand coverage in the pixel
Bare sand	100% bare sand coverage in the pixel
Mixed substrates with red/brown algae	Mixed coverages of seagrass, sand, gravel and macro-algae in the pixel

second one using the R_{rs} data (only atmospheric correction = AC).

To validate and compare the results of both reflectance data sets, we created error matrices. They were the basis to calculate balanced accuracy and F1-Score as overall classification accuracy metrics. Furthermore, we determined class-wise precision and recall using the implemented functions of sklearn (version 0.24.1; Pedregosa et al., 2011). Furthermore, we assessed these accuracies for different water depths. To this end, we categorized the validation data points into 0–1, 1–2, 2–3, 3–4 and >4 m based on the official bathymetric chart.

Additionally, we conducted a McNemar test (python package statsmodels version 0.9.0, Seabold & Perktold, 2010) using the validation data to figure out whether the AC and ACWC classification results are significantly different. As null hypothesis, we assumed that classification disagreements of AC and ACWC are similarly distributed. We used alpha = 0.05 as significance level.

Results

Water column correction

Before obtaining R_b, the water column correction includes three intermediate results, that is R_{deep}, K_d and water depth. R_{deep} was retrieved over a homogenous area in optically deep waters and shows low reflectance intensity, which decreases from blue to near-infrared wavelengths (Fig. 5).

The scatterplots in Fig. 6A show linear relationships between logarithmic R_{rs} and LiDAR water depth based on the sandy subarea, which served to estimate K_d. K_d was estimated according to Equation 2 and increases from blue to red wavelengths (Fig. 6B).

Satellite- and LiDAR-derived water depths scatter around the 1:1 line (Fig. 7). Accuracy measures (R^2 = 0.87, RMSE = 0.20 m) indicate a strong linear relationship with a slight offset, but are satisfactory considering the optically complex water body. The empiric model underestimates water depths larger than 3.5 m, which indicates that we approach the maximum analysable water depth. Additionally, the Sentinel-2 derived water depths show reasonable spatial patterns from the shoreline to deeper waters (Fig. 8) with elevated sand bars interrupting the depth gradient (e.g. Fig. 8 subarea B and C).

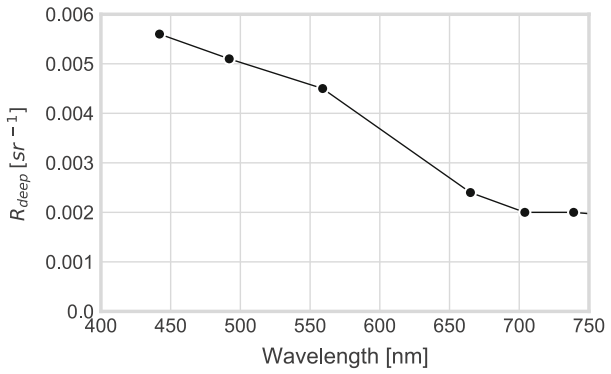

Figure 5. R_{deep} [sr^{-1}] spectrum calculated as the arithmetic mean over a homogenous optically deep water area (6.8 × 3.9 km; blue rectangle in Fig. 1A).

Benthic habitat classification

We delineated five major benthic habitat classes in the study area (Fig. 3, Table 2). Dense seagrass covers most parts of the study area (~25 km²), followed by bare sand (~24.7 km²) and the mixed coverage classes (seagrass dominated: ~7.3 km², sand dominated: ~15.7 km²). When looking at the total areas, the classification results based on R_b (ACWC) and R_{rs} (AC) differed marginally (Fig. 9).

Figure 10 depicts the spatial patterns of mapped coastal benthic habitats. Bare sand predominates close to the shoreline (Fig. 10B). The mixed substrates and algae habitat primarily occurs in the area, where training data were available for this class (Fig. 10A) and appears only occasionally at other places (e.g. Fig. 10C). Seagrass coverage generally increases towards deeper waters interrupted now and then by sand bars. Various patterns can explain the spatial characteristics of *Zostera marina*. Large, dense meadows mainly occur in sheltered bays (Fig. 10A). In areas with coastal sand bar systems (e.g. Fig. 10B and C), dense seagrass clearly aligns along bars and is controlled by troughs and ridges. Anthropogenic structures, such as breakwaters, seem to significantly influence the shape of seagrass meadows (e.g. Fig. 10B). Such spatially explicit and detailed maps of shallow water seagrass distribution can serve as a basis for further geospatial and environmental analyses.

Accuracy assessment

Based on 6942 independent sampling points, we calculated balanced accuracies of 92% based on the entire classification result for both data sets (AC and ACWC). The McNemar test revealed a p-value of 0.09. Thus, we cannot reject the null hypothesis, that is the water column correction did not affect the distribution of disagreements. Similarly, per-class F1-score values were very similar for both AC and ACWC. Bare sand performed best, followed by dense seagrass (Fig. 11). The classes with mixed coverages were less accurate, most probably due to patches where the predominant coverage of sand or seagrass remains unclear. The class 'mixed substrates with red/brown algae' should be handled with caution, since only a few validation points exist for this class (Table 3).

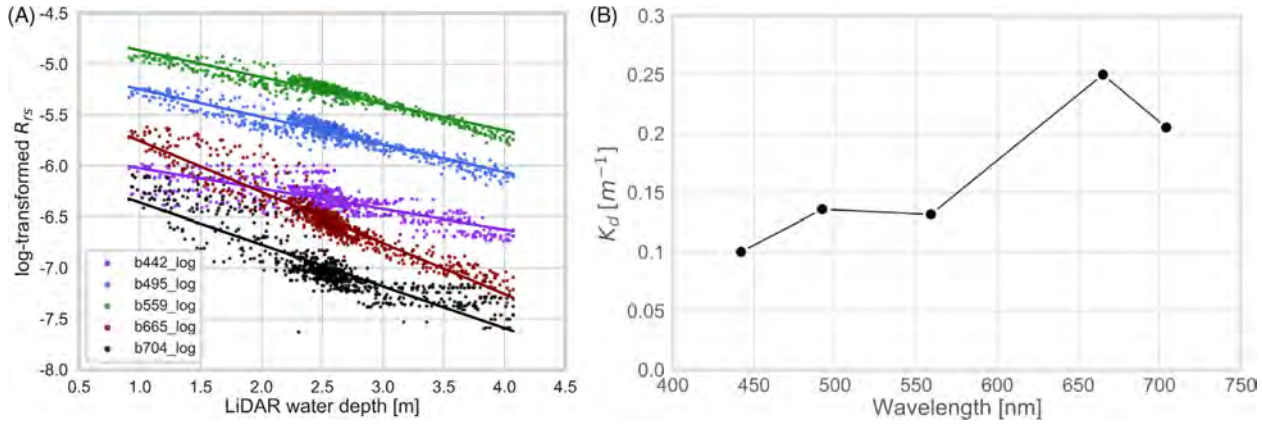

Figure 6. (A) Scatterplot and linear regression lines between log-transformed R_{rs} and LiDAR water depth based on the subregion used for estimating K_d. (B) Band-dependent K_d values calculated from the regression slopes.

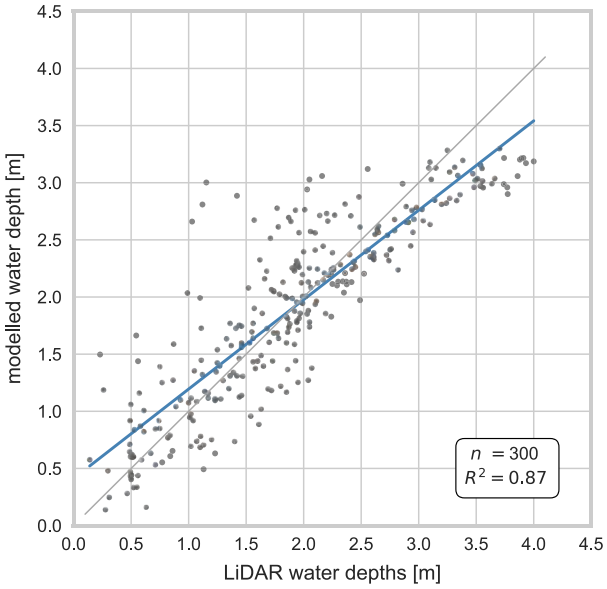

Figure 7. Scatterplot to validate the bathymetric model with independent validation data (n = 300), which was selected randomly from the LiDAR data basis.

When considering depth dependency, bare sand performs best in all depths. Dense seagrass was classified best in water depths >2 m. Since *Zostera marina* mostly grows in water deeper than 1 m, the seagrass classes have a low sampling number (N) in the very shallow waters. The mixed classes dominated by sand or seagrass vary around F1-Score = 0.85 without showing a clear depth-dependency. Mixed substrates with red/ brown algae show similar patterns; they, however, included fewer validation pixels and became very inaccurate below 4 m (Fig. 12A–E).

Independent of the class, the overall classification result was most accurate in very shallow water (<1 m) and for water depths between 2 and 4 m. Balanced accuracy was lowest in water depths >4 m, which may be due to the small sample size.

Discussion

In our study, we aimed at evaluating the potential of Sentinel-2 for mapping coastal benthic habitats in the turbid Baltic Sea using a random forest classifier. In the following, we discuss the results for mapping the dominant benthic habitats, that is dense seagrass, seagrass dominated, sand dominated, bare sand and mixed substrates with red/ brown algae.

How can Sentinel-2 contribute to fill data gaps to map seagrass in shallow, turbid waters?

As a first attempt to map seagrass in the turbid Baltic Sea, our analyses rely on one Sentinel-2 scene. The AC and ACWC derived maps show reasonable spatial patterns of five predominating coastal habitats. Validation results confirm well in water depths between 0 and 5 m, which corresponds with the area, where boat-based mappings become inefficient or impossible. Using optical satellite data, we recommend selecting a scene with good acquisition conditions (relatively clear and calm water, cloud-free) close to the seasonal peak growth during late summer to capture the maximum seagrass habitat area during one year. To follow-up, AC and ACWC approaches need to be analysed using multiple satellite data, for example of consecutive years. Using ACWC, classifying the dynamic coastal sand bars correctly, however, may require timely bathymetric data (at least from the same season).

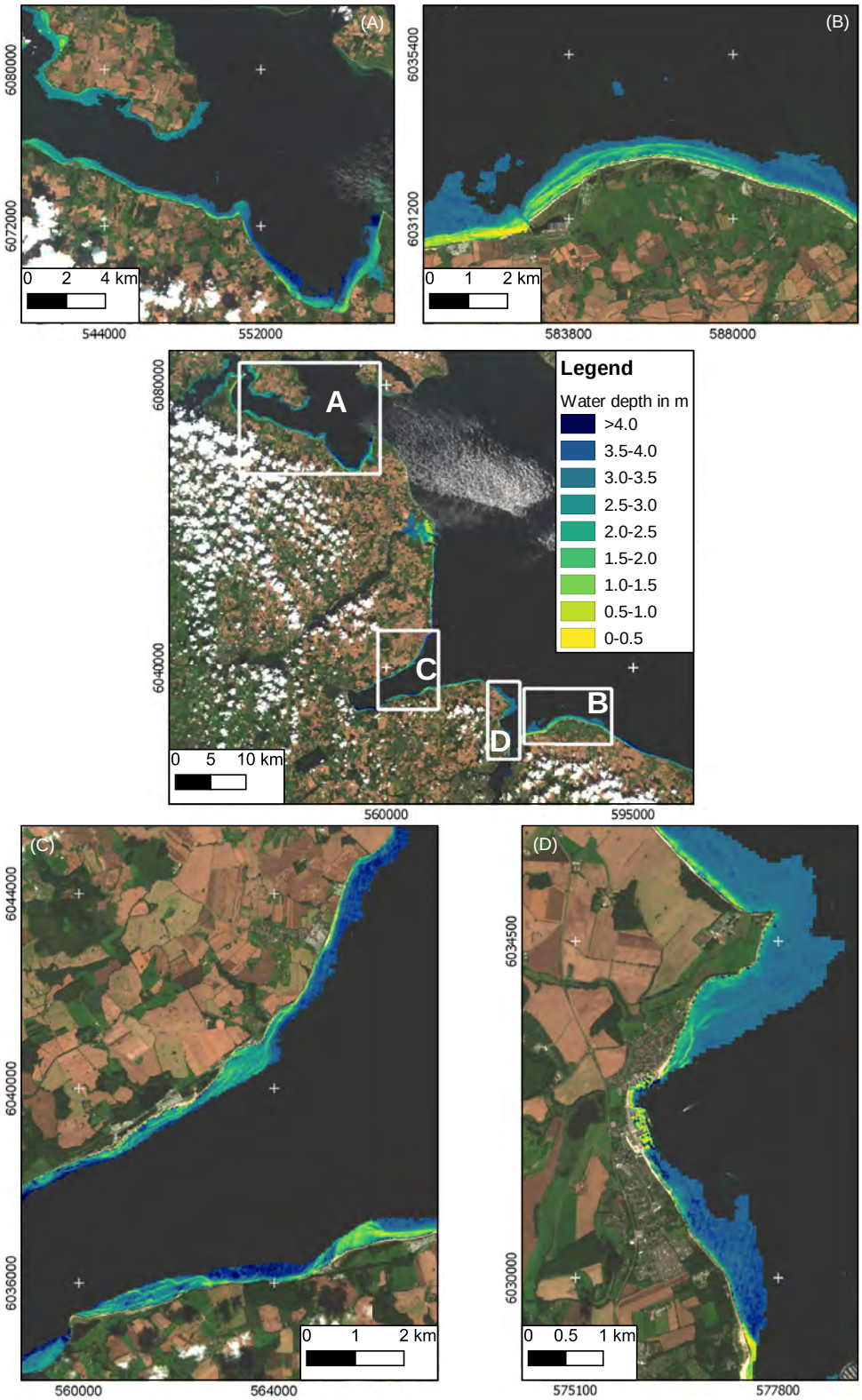

Figure 8. Sentinel-2-derived water depths based on band 4 (665 nm) and the scene-specific bathymetry model. A, B, C and D emphasize four subareas with extended shallow water areas. Background: L1C Sentinel-2B true-colour composite (23 Aug 2017) projected in UTM Zone 32 N/WGS84. Geotiff is available via Zenodo (https://zenodo.org/record/5212257#.YRv4iYgzZaQ; https://doi.org/10.5281/zenodo.5212256).

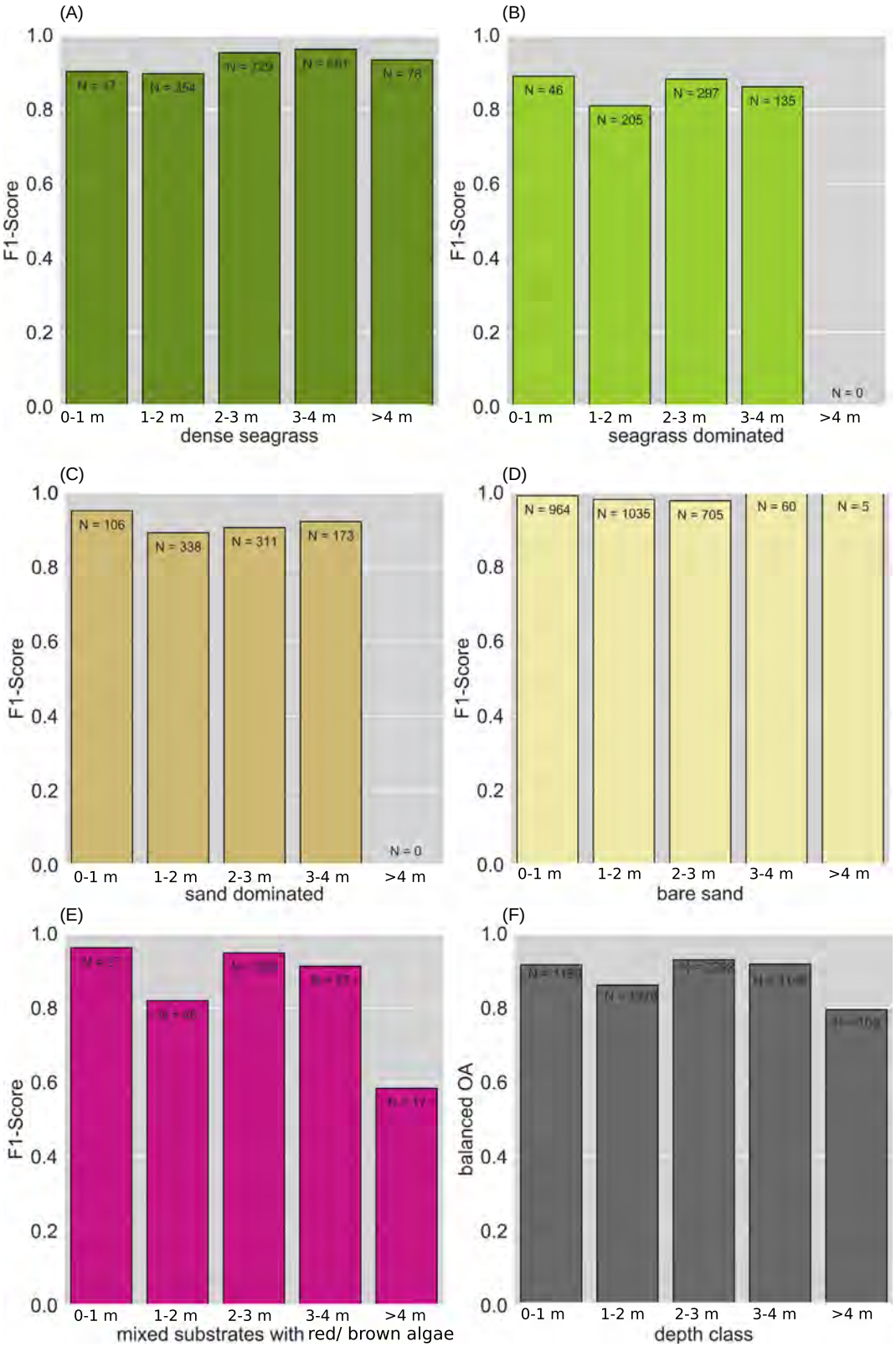

Figure 9. Area of the five benthic habitat classes in the study area based on the AC (based on atmospherically corrected data) and ACWC (based on atmospherically and water column corrected data) classification results in optically shallow water between 0 and 5 m water depth.

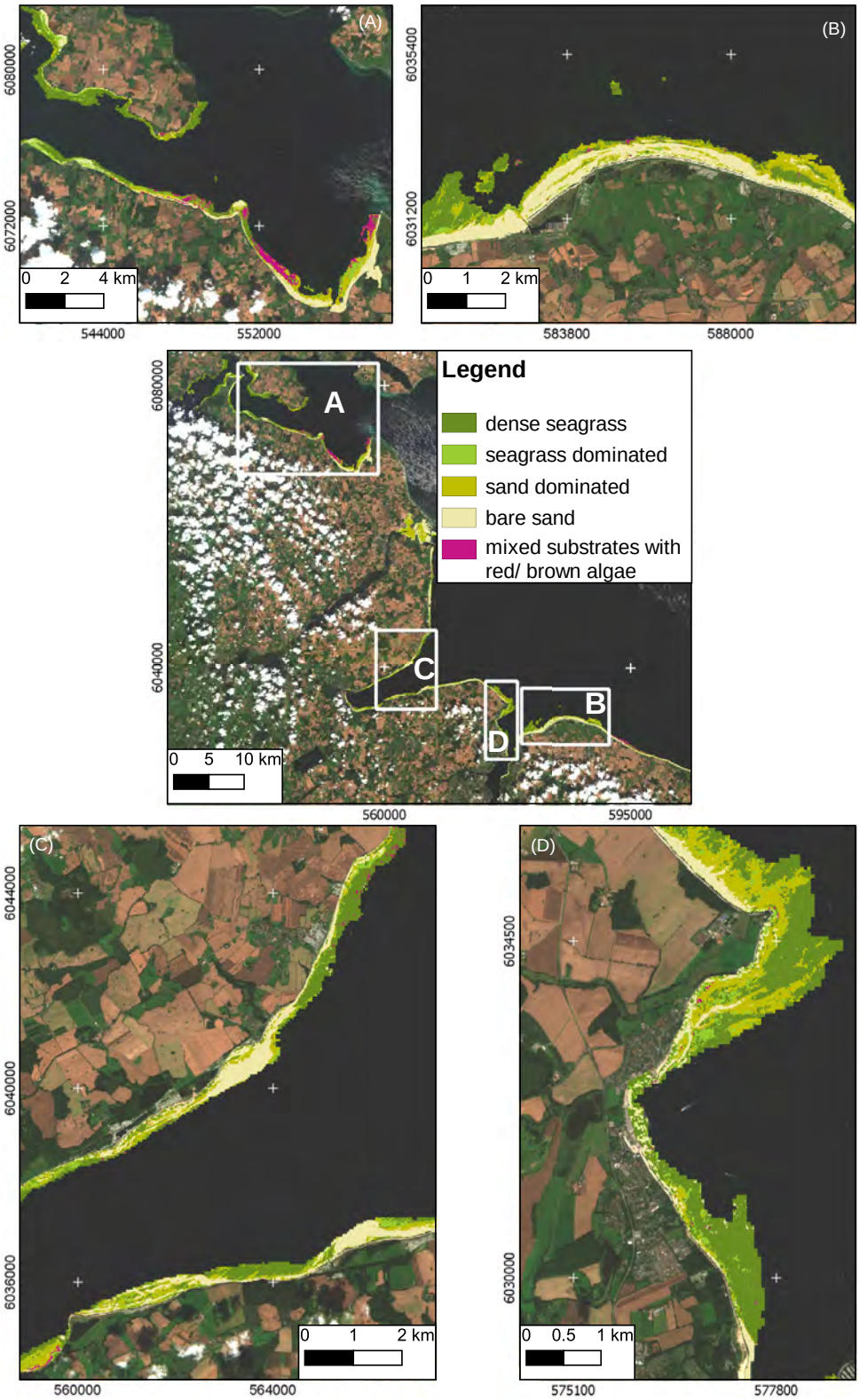

Figure 10. Random forest classification result of coastal benthic habitats based on the R_b data set (ACWC). A, B, C and D emphasize four subareas with extended shallow water areas Background: L1C Sentinel-2B true-colour composite (23 Aug 2017) projected in UTM Zone 32 N/ WGS84. Geotiffs (AC and ACWC) are available via Zenodo (https://zenodo.org/record/5212257#.YRv4iYgzZaQ; https://doi.org/10.5281/zenodo.5212256).

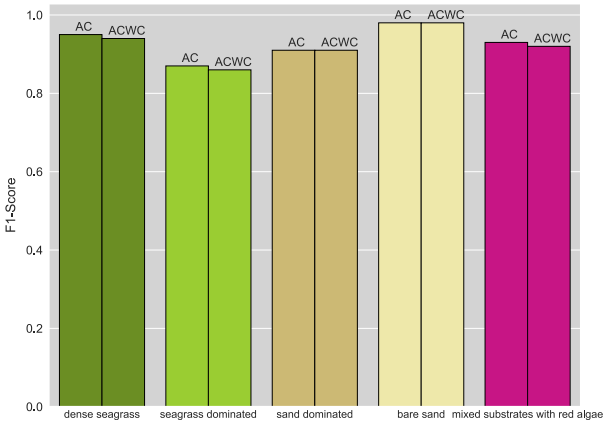

Figure 11. F1-score values per class and for each classification data basis (AC based on R_{rs} data and ACWC based on R_b data).

Zostera marina meadows expand at time scales of several years; rhizomes steadily migrate about 10 cm per year (Boström et al., 2014). With a spatial resolution of 10–20 m, it is hardly possible to capture those gradual changes annually with Sentinel-2. Sudden losses of large meadows, however, may occur within a year and could be probably detected with Sentinel-2. Furthermore, patchiness and fragmentation of seagrass habitats are ecologically highly relevant (Boström et al., 2006). Transect based video mappings cover narrow, 1- to 4-m-wide strips and are a first data basis for calculating such metrics (Schubert et al., 2015). Sentinel-2, however, provides a spatially connected data basis to derive these metrics in shallow waters. The close-up views (Fig. 13) clearly depict the spatial patterns of mapped habitats, for example larger, connected seagrass meadows in sheltered bays (Fig. 13A and B) and fragmented seagrass patches at exposed areas close to anthropogenic coastal protection measures (breakwaters, Fig. 13C). Using these data to calculate landscape metrics requires knowledge on potential classification errors and accuracies.

To this end, direct comparisons between point-based in-situ and satellite seagrass coverage are difficult due to their different spatial scales (Dekker et al., 2011). Additionally, in situ data, in particular interpreted video data, are prone to misinterpretation and not error-free. To overcome the first issue, we implement an upscaling approach with true colour aerial imagery as intermediate scale level. Thus, we create a large database of coastal benthic habitats for calibration and validation. Nevertheless, we are limited to benthic habitats, which can be delineated visually in the aerial imagery and the information from the video transect data. The latter already comprises seagrass coverage values (0–100%), which enables us to classify four seagrass coverage classes (no seagrass = bare sand to dense seagrass >90% coverage). At the Flensburg Fjord (Fig. 10A), we can verify mixed substrates with cobbles, different filamentous algae and partially red and brown macroalgae using the towed video material. However, the limited number of reference pixels, which are also unevenly distributed, hamper validating and training this class confidently. Subsequent analyses should include this class, which is closely related to stone habitats. Stone habitats consist of cobbles and boulders, on which red and brown macroalgae (e.g. *Fucus spp.*) grow (Rönn et al., 2021).

Due to a lack of sufficient reference data, we are unable to clearly state whether Sentninel-2 can spectrally distinguish overgrown stone habitats from seagrass meadows. Sentinel-2 spectra of brown macroalgae and seagrass meadows appear similar in waters (Wilson et al., 2020). Furthermore, Sentinel-2's pixel sizes may capture the narrow, heterogeneous stone habitats close to the shoreline as mixed pixels, which may hamper a further differentiation of the habitats. At the exposed cliff Schönhagen (Fig. 13D), for instance seagrass meadows are absent according to video data from 2010 and 2019. Using Sentinel-2 and the available reference data, both trained random forest models (ACWC, AC) are unable to allocate this habitat correctly and classify the area erroneously as dense seagrass or seagrass dominated (Fig. 13D). Thus, we are aware that the classes dense seagrass and seagrass dominated may include stone habitats. Spatial information on stone habitats, however, is rare although they are

Table 3. Confusion matrix based on the AC and ACWC (AC/ACWC) classification result.

	Class	Dense seagrass	Seagrass dominated	Sand dominated	Bare sand	Mixed substrates with red/ brown algae
		Classified				
True	Dense seagrass	1923/1922	46/42	32/32	8/10	11/11
	Seagrass dominated	59/66	593/570	26/32	10/9	5/6
	Sand dominated	15/20	27/20	863/861	37/39	0/2
	Bare sand	15/12	1/3	26/26	2809/2810	0/0
	Mixed substrates with red/ brown algae	31/42	5/5	3/3	0/0	404/396

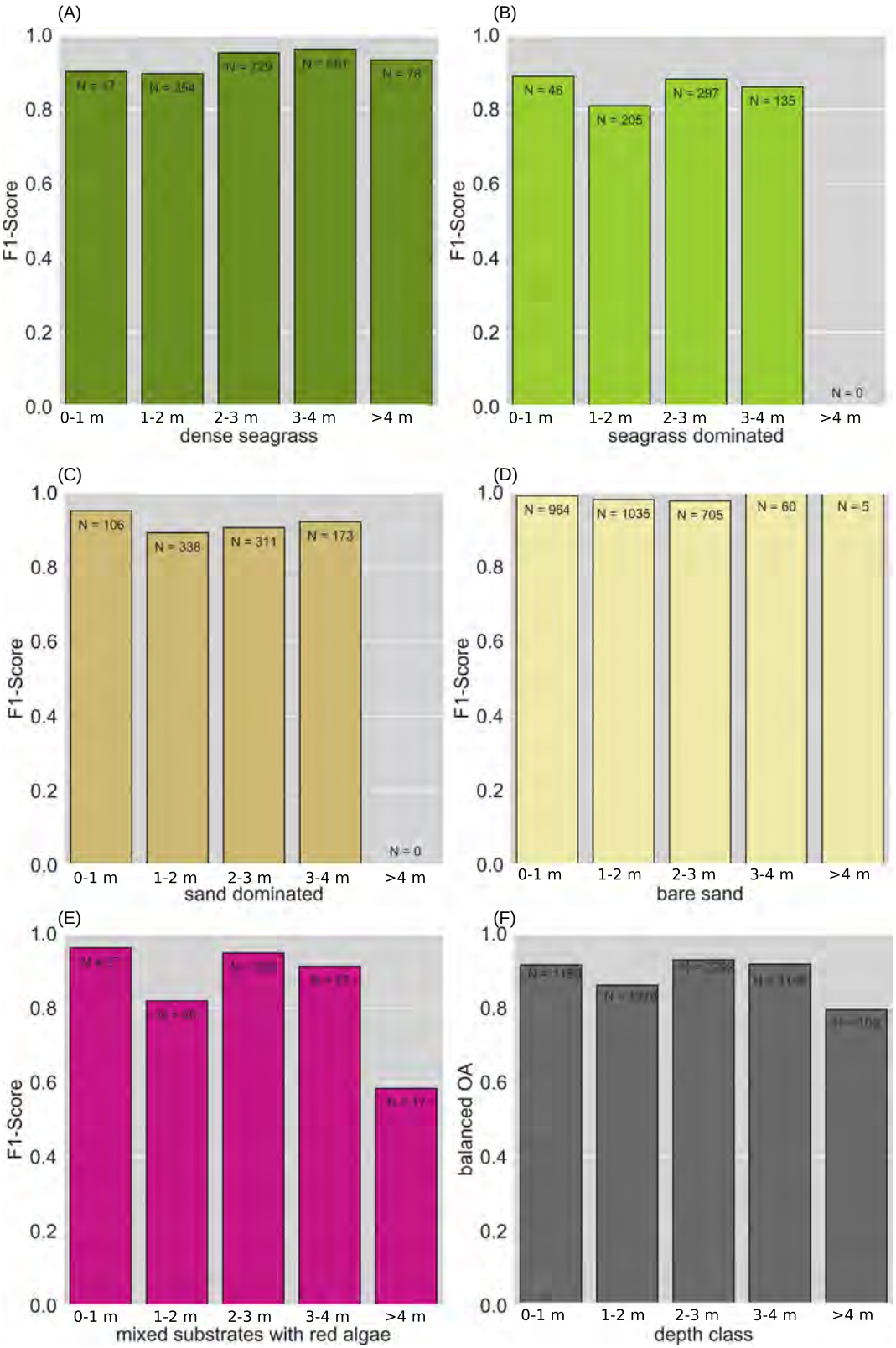

Figure 12. F1-Score values (ACWC) for each class divided according to 1 m water depth steps (A–E). Balanced accuracy (ACWC) calculated based on all classes divided according to 1 m water depth steps (F). Note the varying sampling sizes (N) in the different depth steps.

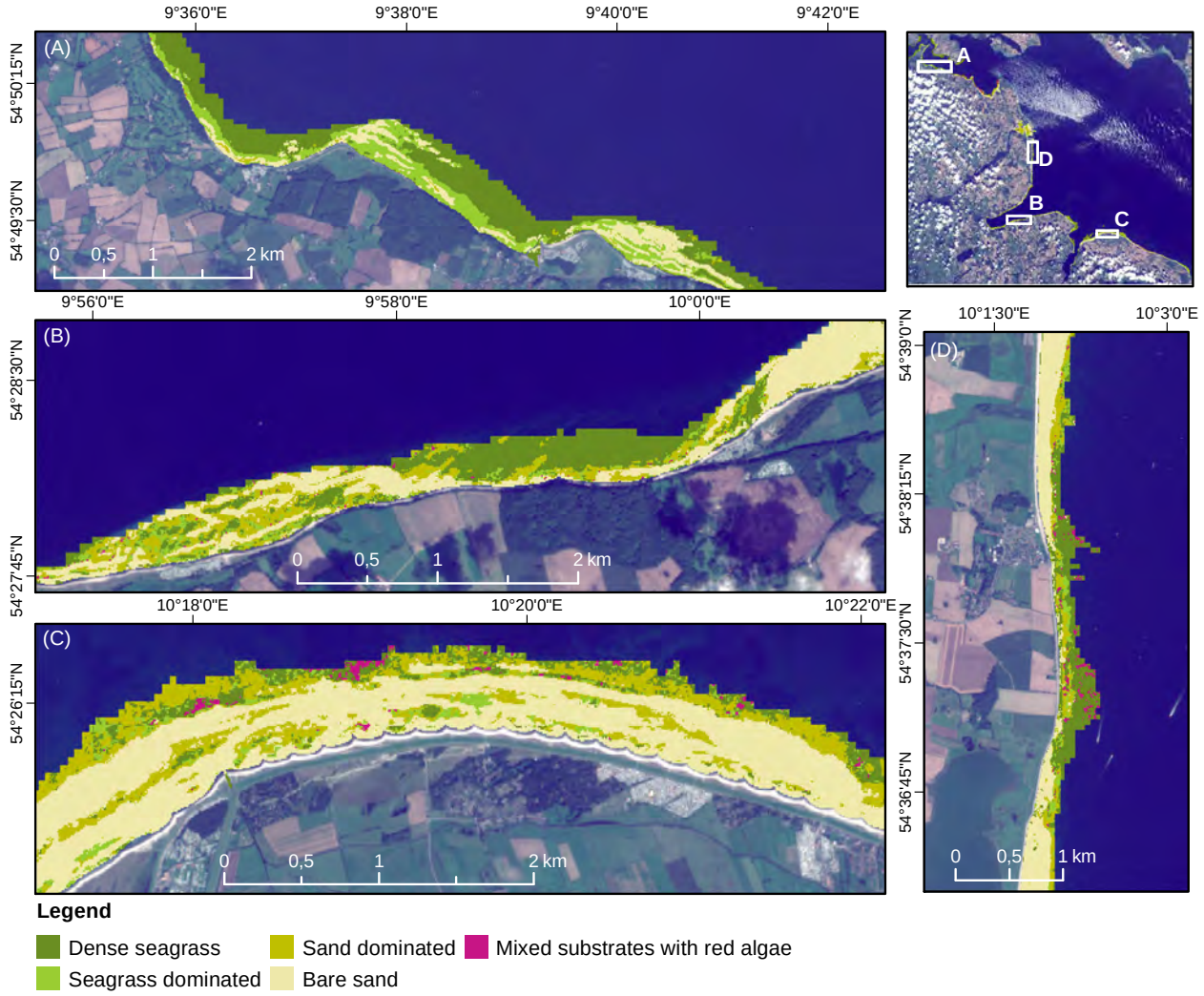

Figure 13. Close-up views of ACWC classification results at Flensburg Fjord (A), Eckernförde Fjord (B), Heidkate (C) and Cliff Schönhagen (D). Background: L1C Sentinel-2B true-colour composite (23 Aug 2017) projected in UTM Zone 32 N/ WGS84.

biodiversity hotspots and should be considered for marine habitat monitoring (Rönn et al., 2021). Thus, it is worth collecting field spectra and locations of stone habitats to examine whether we can further distinguish coastal habitats with Sentinel-2 in the Baltic Sea, using for instance spectral unmixing approaches.

Do we need a water column correction to map seagrass accurately?

Using the same calibration data, we trained two random forest classification models, one for the R_b (ACWC) and one for the R_{rs} (AC) data. The resulting spatial distributions of habitat classes differed only marginally (up to 0.3 km²). Individual pixels at the edge of habitat patches were differently classified, but systematic differences were absent and statistically insignificant (P-value = 0.09). The same applies to the quantitative validation, which actually is reasonable. The available calibration data perfectly train the random forest models to the conditions and values in the R_b and R_{rs} data. Consequently, they perform similarly; adversely, as data-driven models, they are hardly transferable to other image acquisitions with different conditions (Belgiu & Drăguţ, 2016). In particular, the R_{rs} data should compensate varying atmospheric conditions, since ACOLITE corrects atmospheric influences and partially water surface effects (sun glint). Varying water column conditions, such as suspended matter or chlorophyll-a concentrations, remain unaddressed. Therefore, the water column corrected data might be better suited to transfer a random forest model to other image acquisitions. The here adopted approach to correct the water column either

needs a timely bathymetric chart or known bathymetry points to calibrate an image-based water depth model.

Marginal accuracy differences between AC and ACWC classification results indicate that it might be sufficient to conduct an atmospheric correction to classify benthic habitats satisfactorily. Similarly, Poursanidis et al., 2018 found that water column correction hardly influences the results of classified Mediterranean coastal marine habitats using WorldView-2 data. Our finding, however, should be restricted to single image analyses based on optimal water conditions (calm surface, lowest turbidity). With and without, water column correction, we are able to delineate five major benthic habitats. This knowledge allows mapping benthic habitats in areas where timely bathymetry data are absent. Recent computing capacities allow training a machine-learning classifier with low effort to individual scenes and study areas. Nevertheless, we need training and validation data of benthic habitat classes, which are comparable to the acquisition conditions of a satellite scene.

How do classification accuracies vary with water depth?

The deeper the water column, the more radiation it absorbs. With decreasing water reflectance, benthic habitat classes can be separated less accurately (Malthus, 2017). We, therefore, expected that classification accuracies impair with increasing water depths. Indeed, the balanced accuracy of the entire classification is worst for the deepest water depth category (>4 m). The low performance, however, may also be due to the small sample size. Between 0 and 4 m, class-dependent accuracies vary but lack any clear depth-dependency. Bare sand reflects strongly compared to the other classes and is therefore clearly separable in all water depths (F1-score close to 100%). In contrast, dense seagrass is unlikely to occur widespread in very shallow water (<1 m; low N). Dense seagrass further may mix up with other coverage classes (e.g. seagrass dominated), which could explain the lower performance in depths between 1 and 2 m.

In summary, the depth-dependent validation indicates that accuracies appear to be independent of the water depth. This is promising for a Sentinel-2 based benthic habitat mapping in shallow waters. Nevertheless, masking optically deep water remains critical because reflectance spectra of optically deep water are hardly separable from dense seagrass spectra.

With offshore Secchi disc depths around 5–6 m during the summer months, we set the optically shallow water depth limit to 5 m. Visual comparisons between the bathymetric contour and the R_b/ R_{rs} data confirm that limit. Nevertheless, episodic resuspension or algal blooms in nearshore areas may reduce the detection limit locally, while the opposite is true for upwelling events following strong offshore winds or clear water phases between algal blooms. In water depths >5 m, classifying pixels into benthic habitats is highly inaccurate. Therefore, we suggest concentrating on water depths <5 m for Sentinel-2 based benthic habitat classifications in the Western Baltic Sea.

Conclusions

The spatial resolution of Sentinel-2 allows investigating shallow coastal areas. This study on seagrass habitats in the Baltic Sea emphasizes that Sentinel-2 can confidentially deliver information on seagrass habitats in turbid waters between 0 and 5 m with straightforward, image-based classification methods. Thus, the sensor can contribute important data to the data-scarce coastal white ribbon. The currently distinguishable classes are a step further from the former presence or absence data for vegetation. Better delineating stone habitats and transferring the image-based approaches temporally should be the next challenge.

Seagrass in the Western Baltic Sea was reported to occur down to 7.6 m (Schubert et al., 2015), compared to 14 m some decades ago (Schramm, 1996). Although optical methods perform well in shallow waters, significant parts of seagrass habitats grow in optically deep water. Recent research in our study area disclosed that multibeam acoustic methods together with machine leaning approaches can reliably map *Zostera marina* beyond 5 m (Held & Schneider von Deimling, 2019). Envisioning a holistic and extensive seagrass mapping, we propose a synoptic opto-acoustic approach, which combines optical satellite data and ship-borne acoustical surveying to obtain a comprehensive picture of seagrass habitat extents and dynamics.

Acknowledgements

This study was developed within a project financed by Kiel Marine Science to connect different research groups at Kiel University (Grant KMS1701). We thank Dr. Rolf Karez (LLUR; State agency for Agriculture, Environment and Rural Areas) for kindly providing the seagrass video transect data and his never fading interest in seagrass. Many thanks to our student assistants Victor Lion and Max Jakob Martius, who helped to create result figures and maps. Furthermore, we thank ESA (European Space Agency) to provide Sentinel-2 data with free access. Many thanks to the two reviewers for providing helpful comments.

Authors' Contributions

Katja Kuhwald, Natascha Oppelt (remote sensing part) and Jens Schneider von Deimling (seagrass and

bathymetry mapping) conceived and designed the study. Jens Schneider von Deimling provided the LiDAR data and discussion points on seagrass mapping in the Baltic Sea. Philipp Schubert contributed the video mapping data and provided insights into local benthic habitats. Katja Kuhwald implemented and conducted the remote sensing image processing and wrote the first draft of the manuscript. All authors contributed in revising and finalising the manuscript.

Funding information

This study was funded by Kiel Marine Science, the Centre for Interdisciplinary Research at Kiel University under grant KMS1701 and was supported by the BONUS project ECOMAP (Art 185), funded jointly by the EU and the Federal Ministry of Education and Research of Germany (BMBF), the National Centre for Research and Development of Poland (NCBR) and the Innovation Fund Denmark (Innovationsfonden). Acquisition of video data was funded by the LLUR.

References

Belgiu, M. & Drăguţ, L. (2016) Random forest in remote sensing: a review of applications and future directions. *ISPRS Journal of Photogrammetry and Remote Sensing*, **114**, 24–31.

Bierwirth, P.N., Lee, T.J. & Burne, R.V. (1993) Shallow sea-floor reflectance and water depth derived by unmixing multispectral imagery. *Photogrammetric Engineering and Remote Sensing*, **59**, 331–338.

Borum, J., Duarte, C.M., Greve, T.M. & Krause-Jensen, D. (2004) European seagrasses: An introduction to monitoring and management. The M & MS project, [Erscheinungsort nicht ermittelbar].

Boström, C., Baden, S., Bockelmann, A.-C., Dromph, K., Fredriksen, S., Gustafsson, C. et al. (2014) Distribution, structure and function of Nordic eelgrass (Zostera marina) ecosystems: Implications for coastal management and conservation. *Aquatic Conservation : Marine and Freshwater Ecosystems*, **24**(3), 410–434.

Boström, C., Jackson, E.L. & Simenstad, C.A. (2006) Seagrass landscapes and their effects on associated fauna: a review. *Estuarine, Coastal and Shelf Science*, **68**(3–4), 383–403.

BSH (2012) Official Baltic Sea Bathymetry Database. 50 m horizontal spatial resolution. Bundesamt für Seschifffahrt und Hydrographie (BSH)

Carvalho, R.C., Hamylton, S. & Woodroffe, C.D. (2017) Filling the 'white ribbon' in temperate Australia: A multi-approach method to map the terrestrial-marine interface. In 2017 IEEE/OES Acoustics in Underwater Geosciences Symposium: RIO Acoustics 2017 : Rio de Janeiro, Brazil, July 25-27, 2017, pp. 1–5. IEEE, Piscataway, NJ.

Casal, G., Monteys, X., Hedley, J., Harris, P., Cahalane, C. & McCarthy, T. (2018) Assessment of empirical algorithms for bathymetry extraction using Sentinel-2 data. *International Journal of Remote Sensing*, **40**(8), 2855–2879.

de los Santos, C.B., Krause-Jensen, D., Alcoverro, T., Marbà, N., Duarte, C.M., van Katwijk, M.M. et al. (2019) Recent trend reversal for declining European seagrass meadows. *Nature Communications*, **10**(1), 3356.

Dekker, A.G., Phinn, S.R., Anstee, J.M., Bissett, W.P., Brando, V.E., Casey, B. et al. (2011) Intercomparison of shallow water bathymetry, hydro-optics, and benthos mapping techniques in Australian and Caribbean coastal environments. *Limnology and Oceanography: Methods*, **9**, 396–425.

Drusch, M., Del Bello, U., Carlier, S., Colin, O., Fernandez, V., Gascon, F. et al. (2012) Sentinel-2: ESA's optical high-resolution mission for GMES operational services. *Remote Sensing of Environment*, **120**, 25–36.

Gege, P. (2017) Radiative transfer theory for inland waters. In: Mishra, D.R., Ogashawara, I. & Gitelson, A.A. (Eds.) *Bio-optical modeling and remote sensing of inland waters*. Amsterdam: Elsevier.

Gumusay, M.U., Bakirman, T., Tuney Kizilkaya, I. & Aykut, N.O. (2019) A review of seagrass detection, mapping and monitoring applications using acoustic systems. *European Journal of Remote Sensing*, **52**(1), 1–29.

Harmel, T., Chami, M., Tormos, T., Reynaud, N. & Danis, P.-A. (2017) Sunglint correction of the Multi-Spectral Instrument (MSI)-SENTINEL-2 imagery over inland and sea waters from SWIR bands. *Remote Sensing of Environment*, **204**, 308–321. https://doi.org/10.1016/j.rse.2017.10.022.

Held, P. & Schneider von Deimling, J. (2019) New feature classes for acoustic habitat mapping—A multibeam echosounder point cloud analysis for mapping submerged aquatic vegetation (SAV). *Geosciences*, **9**(5), 235.

Kirk, J.T.O. (2011) *Light and photosynthesis in aquatic ecosystems*. Cambridge, UK, New York: Cambridge University Press.

Kovacs, E., Roelfsema, C., Lyons, M., Zhao, S. & Phinn, S. (2018) Seagrass habitat mapping: how do Landsat 8 OLI, Sentinel-2, ZY-3A, and Worldview-3 perform? *Remote Sensing Letters*, **9**(7), 686–695.

Kratzer, S. & Moore, G. (2018) Inherent optical properties of the baltic sea in comparison to other seas and oceans. *Remote Sensing*, **10**(3), 418.

Krause-Jensen, D., Duarte, C.M., Sand-Jensen, K. & Carstensen, J. (2021) Century-long records reveal shifting challenges to seagrass recovery. *Global Change Biology*, **27**(3), 563–575.

Lamb, J.B., van de Water, J.A.J.M., Bourne, D.G., Altier, C., Hein, M.Y., Fiorenza, E.A. et al. (2017) Seagrass ecosystems reduce exposure to bacterial pathogens of humans, fishes, and invertebrates. *Science*, **355**(6326), 731–733.

Lovelock, C.E. & Duarte, C.M. (2019) Dimensions of Blue Carbon and emerging perspectives. *Biology Letters*, **15**(3), 20180781.

LVermGeo SH (2016) GeoBasis-DE/LVermGeo SH (http://www.schleswig-holstein.de/DE/GDISH/gdish_node.html) data basis: ATKIS®-DOP20. Landesamt für Vermessung und Geoinformation Schleswig-Holstein (LVermGeo SH).

Lyons, M.B., Roelfsema, C.M. & Phinn, S.R. (2013) Towards understanding temporal and spatial dynamics of seagrass landscapes using time-series remote sensing. *Estuarine, Coastal and Shelf Science*, **120**, 42–53.

Madden, C.J., Rudnick, D.T., McDonald, A.A., Cunniff, K.M. & Fourqurean, J.W. (2009) Ecological indicators for assessing and communicating seagrass status and trends in Florida Bay. *Ecological Indicators*, **9**(6), S68–S82.

Malthus, T.J. (2017) Bio-optical modeling and remote sensing of aquatic macrophytes. In: Mishra, D.R., Ogashawara, I. & Gitelson, A.A. (Eds.) *Bio-optical modeling and remote sensing of inland waters*. Amsterdam: Elsevier, pp. 263–308.

Marbà, N., Krause-Jensen, D., Alcoverro, T., Birk, S., Pedersen, A., Neto, J.M. et al. (2013) Diversity of European seagrass indicators: patterns within and across regions. *Hydrobiologia*, **704**(1), 265–278.

Maritorena, S., Morel, A. & Gentili, B. (1994) Diffuse reflectance of oceanic shallow waters: influence of water depth and bottom albedo. *Limnology and Oceanography*, **39**(7), 1689–1703.

McKenzie, L.J., Nordlund, L.M., Jones, B.L., Cullen-Unsworth, L.C., Roelfsema, C. & Unsworth, R.K.F. (2020) The global distribution of seagrass meadows. *Environmental Research Letters*, **15**(7), 74041.

MELUND (2017). Monitoring data of the coastal water measurement site 'Kolberger heide'. ID: 225090. Ministerium für Energiewende, Landwirtschaft, Umwelt, Natur und Digitalisierung Schleswig-Holstein (MELUND.).

Niemeyer, J., Song, Y., Kogut, T. & Heipke, C. (2015). Untersuchungen zum Einsatz der Laserbathymetrie in der Seevermessung. Project Report (Federal Hydrographic Agency BSH, Germany).

Orth, R.J., Carruthers, T.J.B., Dennison, W.C., Duarte, C.M., Fourqurean, J.W., Heck, K.L. et al. (2006) A global crisis for seagrass ecosystems. *BioScience*, **56**(12), 987.

Pedregosa, F., Varoquax, G., Gramfort, A., Michel, V., Thirion, B., Grisel, O. et al. (2011) Scikit-learn: machine learning in Python. *Journal of Machine Learning Research*, **12**(85), 2825–2830.

Perry, M. (2020). Pyimpute: Utilities for applying scikit-learn to spatial datasets.

Poursanidis, D., Topouzelis, K. & Chrysoulakis, N. (2018) Mapping coastal marine habitats and delineating the deep limits of the Neptune's seagrass meadows using very high resolution Earth observation data. *International Journal of Remote Sensing*, **39**(23), 8670–8687.

Reinke, J. (1889) Algenflora der westlichen Ostsee deutschen Antheils. Eine systematisch-pflanzengeographische Studie. In: *Ein Bericht der Kommission zur Wissenschaftlichen Untersuchung der Deutschen Meere in Kiel*. III-XI, 1–101. Schmidt & Klaunig, Kiel.

Reusch, T.B.H., Dierking, J., Andersson, H.C., Bonsdorff, E., Carstensen, J., Casini, M. et al. (2018) The Baltic Sea as a time machine for the future coastal ocean. *Science Advances*, **4**(5):eaar8195.

Ricart, A.M., York, P.H., Bryant, C.V., Rasheed, M.A., Ierodiaconou, D. & Macreadie, P.I. (2020) High variability of Blue Carbon storage in seagrass meadows at the estuary scale. *Scientific Reports*, **10**, 5865. https://doi.org/10.1038/s41598-020-62639-y

Schneider von Deimling, J. (2020). BONUS ECOMAP – Baltic Sea environmental assessments by innovative opto-acoustic remote sensing, mapping, and monitoring. Final scientific report.

Schramm, W. (1996) *The baltic sea and its transition zones*. Berlin Heidelberg: Springer.

Schubert, P.R., Hukriede, W., Karez, R. & Reusch, T.B.H. (2015) Mapping and modeling eelgrass Zostera marina distribution in the western Baltic Sea. *Marine Ecology Progress Series*, **522**, 79–95.

Seabold, S. & Perktold, J. (2010) statsmodels: Econometric and statistical modeling with python. Proceedings of the 9th Python in Science Conference.

Short, F., Carruthers, T., Dennison, W. & Waycott, M. (2007) Global seagrass distribution and diversity: a bioregional model. *Journal of Experimental Marine Biology and Ecology*, **350**(1–2), 3–20.

Short, F.T., Short, C.A. & Novak, A.B. (2016) *Seagrasses*. Netherlands: Springer.

Snoeijs-Leijonmalm, P. & Andrén, E. (2017) *Why is the Baltic Sea so special to live in?*. Netherlands: Springer.

Stock, A. (2015) Satellite mapping of Baltic Sea Secchi depth with multiple regression models. *International Journal of Applied Earth Observation and Geoinformation*, **40**(3), 55–64.

Thomas, N., Pertiwi, A.P., Traganos, D., Lagomasino, D., Poursanidis, D., Moreno, S. et al. (2021) Space-borne cloud-native satellite-derived bathymetry (SDB) models using ICESat-2 And Sentinel-2. *Geophysical Research Letters* **48**(6):1027.

Topouzelis, K., Makri, D., Stoupas, N., Papakonstantinou, A. & Katsanevakis, S. (2018) Seagrass mapping in Greek territorial waters using Landsat-8 satellite images. *International Journal of Applied Earth Observation and Geoinformation*, **67**, 98–113.

Traganos, D., Aggarwal, B., Poursanidis, D., Topouzelis, K., Chrysoulakis, N. & Reinartz, P. (2018) Towards global-scale seagrass mapping and monitoring using sentinel-2 on google earth engine: the case study of the aegean and ionian seas. *Remote Sensing*, **10**, 1227.

Traganos, D. & Reinartz, P. (2017) Mapping Mediterranean seagrasses with Sentinel-2 imagery. *Marine Pollution Bulletin*, **134**, 197–209. https://doi.org/10.1016/j.marpolbul.2017.06.075.

Traganos, D. & Reinartz, P. (2018) Machine learning-based retrieval of benthic reflectance and Posidonia oceanica seagrass extent using a semi-analytical inversion of Sentinel-2 satellite data. *International Journal of Remote Sensing*, **39** (24), 9428–9452.

UNEP (2020) Out of the blue—The value of seagrasses to the environment and people. UNEP (United Nations Environment Programme), Nairobi.

Vanhellemont, Q. (2019) Adaptation of the dark spectrum fitting atmospheric correction for aquatic applications of the Landsat and Sentinel-2 archives. *Remote Sensing of Environment*, **225**, 175–192.

Veettil, B.K., Ward, R.D., Lima, M.D.A.C., Stankovic, M., Hoai, P.N. & Quang, N.X. (2020) Opportunities for seagrass research derived from remote sensing: a review of current methods. *Ecological Indicators*, **117**(7), 106560.

von Rönn, G.A., Krämer, K., Franz, M., Schwarzer, K., Reimers, H.-C. & Winter, C. (2021) Dynamics of stone habitats in coastal waters of the southwestern baltic sea (Hohwacht Bay). *Geosciences*, **11**(4), 171.

Waycott, M., Duarte, C.M., Carruthers, T.J.B., Orth, R.J., Dennison, W.C., Olyarnik, S. et al. (2009) Accelerating loss of seagrasses across the globe threatens coastal ecosystems. *Proceedings of the National Academy of Sciences of the United States of America*, **106**(30), 12377–12381.

Wilson, K.L., Wong, M.C. & Devred, E. (2020) Branching algorithm to identify bottom habitat in the optically complex coastal waters of atlantic canada using sentinel-2 satellite imagery. *Frontiers in Environmental Science*, **8**, 169.

Zoffoli, M.L., Gernez, P., Rosa, P., Le Bris, A., Brando, V.E., Barillé, A.-L. et al. (2020) Sentinel-2 remote sensing of Zostera noltei-dominated intertidal seagrass meadows. *Remote Sensing of Environment*, **251**(5), 112020.

